

Accepted Manuscript

The Different Perspectives of Internal Carotid Artery in Transnasal Endoscopic Surgery

Davide Mattavelli, MD, Andrea Bolzoni Villaret, MD, Marco Ferrari, MD, Marco Ravanelli, MD, Vittorio Rampinelli, MD, Davide Lancini, MD, Luigi Fabrizio Rodella, MD, Marco Fontanella, MD, Roberto Maroldi, MD, Piero Nicolai, MD, Francesco Doglietto, MD, PhD

PII: S1878-8750(16)30685-4

DOI: [10.1016/j.wneu.2016.08.019](https://doi.org/10.1016/j.wneu.2016.08.019)

Reference: WNEU 4429

To appear in: *World Neurosurgery*

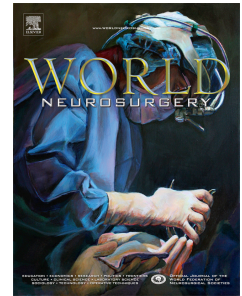
Received Date: 4 April 2016

Revised Date: 3 August 2016

Accepted Date: 5 August 2016

Please cite this article as: Mattavelli D, Villaret AB, Ferrari M, Ravanelli M, Rampinelli V, Lancini D, Rodella LF, Fontanella M, Maroldi R, Nicolai P, Doglietto F, The Different Perspectives of Internal Carotid Artery in Transnasal Endoscopic Surgery, *World Neurosurgery* (2016), doi: 10.1016/j.wneu.2016.08.019.

This is a PDF file of an unedited manuscript that has been accepted for publication. As a service to our customers we are providing this early version of the manuscript. The manuscript will undergo copyediting, typesetting, and review of the resulting proof before it is published in its final form. Please note that during the production process errors may be discovered which could affect the content, and all legal disclaimers that apply to the journal pertain.



THE DIFFERENT PERSPECTIVES OF INTERNAL CAROTID ARTERY IN TRANSNASAL ENDOSCOPIC SURGERY

Davide Mattavelli, MD^a; Andrea Bolzoni Villaret, MD^a; Marco Ferrari, MD^a; Marco Ravanelli, MD^b; Vittorio Rampinelli, MD^a; Davide Lancini, MD^a; Luigi Fabrizio Rodella, MD^d; Marco Fontanella, MD^c; Roberto Maroldi, MD^b; Piero Nicolai, MD^a; Francesco Doglietto, MD, PhD^c

Units of Otorhinolaryngology - Head and Neck Surgery^a, Radiology^b and Neurosurgery^c,
Department of Surgical Specialties, Radiological Sciences, and Public Health, University of
Brescia, Italy

^dSection of Anatomy and Physiopathology, Department of Clinical and Experimental
Sciences, University of Brescia, Italy

Short title: ICA geometry and its endoscopic perception

Key words: carotid, complications, endoscopic surgery, skull base, nasopharyngectomy

Financial disclosures and conflicts of interest: none.

Corresponding author:

Mattavelli Davide, MD

Unit of Otorhinolaryngology- Head and Neck Surgery, Department of Surgical Specialties,
Radiological Sciences, and Public Health, University of Brescia

Piazzale Spedali Civili 1, 25100 Brescia, Italy

Telephone number: +39 0303995319

FAX number: +39 0303996142

Mail address: davide_mattavelli85@yahoo.it

Abbreviations list

AI: angle of incidence

(CB)CT: (cone-beam) computed tomography

contra-AI: contralateral transnasal corridor

EEA: expanded endonasal approach

ICA: internal carotid artery

ipsi-AI: ipsilateral transnasal corridor

NER: nasopharyngeal endoscopic resection

PCA: petrous carotid angle

TES: transnasal endoscopic surgery

TM-ipsi-AI: transmaxillary ipsilateral corridor

Abstract

Background: Several endoscopic landmarks for the internal carotid artery have been identified, but they have always been proposed in a “static” perspective. The aim of this study was to investigate how the surgical corridor and optical distortion can influence the perception of carotid landmarks in transnasal endoscopic surgery.

Methods: Computed tomography images of the skull of 20 subjects were analyzed. The petrous carotid angle (PCA) was calculated as the angle between the petrous carotid axis and the coronal plane connecting stylomastoid foramina. The angle of incidence (AI) on the anterior carotid genu of 3 different surgical corridors (contralateral nostril, ipsilateral nostril, and transmaxillary ipsilateral route) was evaluated. PCA, AI, and their differences were studied by Spearman’s correlation test. Two cadaver heads were dissected, simulating the studied surgical corridors. The fisheye effect was empirically quantified.

Results: Mean PCA was 31°(range, 21-41°). PCA and AI are linked by an inverse proportion relationship. A transmaxillary approach always assures the highest value of AI on the target. The cadaveric dissection qualitatively confirmed the radiological data. The fisheye effect can cause a compression of distance perception as high as 37%.

Conclusions: The surgical corridor and endoscope optic distortion can influence ICA visualization and the perception of its anatomical landmarks. In a 2 nostril-4 handed approach, it is advisable to place the endoscope and instrument for dissection in the nostril that is ipsilateral to the lesion. Awareness of the different perspectives and related optical distortions is essential when working in proximity to the ICA.

Introduction

In the last decades, transnasal endoscopic surgery (TES) has revolutionized the treatment of sinonasal and skull base diseases by enabling a minimally invasive access to complex and deeply located regions. “Expanded endonasal approaches” (EEAs) to the skull base and upper parapharyngeal space have been described in detail and standardized¹⁻³ as an alternative to many classical transcranial approaches. Likewise, nasopharyngeal endoscopic resection (NER) has been added to the surgical armamentarium for the treatment of selected primary and recurrent malignant tumors of this site.⁴⁻⁷

The validation of reliable surgical landmarks for the endoscopic endonasal identification of relevant nervous and vascular structures (i.e., the internal carotid artery [ICA]) has played a pivotal role in the evolution of TES. However, the relationships among anatomical landmarks and ICA has always been studied and proposed in a “static” perspective, without taking into account the importance of the angle of view of the surgical field.

The primary aim of this study was to define the geometry of ICA in its parapharyngeal, petrous, and paraclival components, and explore the influence of the angle of incidence of different surgical corridors on the perception of anatomical landmarks. Furthermore, the impact of the fisheye effect on endoscopic visualization was estimated.

Materials and methods

Radiological study

Twenty consecutive cone-beam computed tomography (CBCT) studies of sinonasal tract and skull base were retrieved from the database of the Department of Radiology, University of Brescia, excluding patients younger than 18 years or with sinonasal and skull base disease. CBCT studies were performed on a Newtom 5G scanner (QR, Verona, Italy) with a field of view of 15x12 cm and isotropic spatial resolution of 200 μm . All patients gave written informed consent for CBCTs, which were performed for clinical purposes.

Image datasets were anonymized before the analysis. Multiplanar reconstructions were used for the following measurements:

1) Petrous carotid angle (PCA), defined as the medial angle between the coronal plane passing through stylomastoid foramina and the plane passing through the anterior and posterior genu of the ICA (fig. 1).

2) Angle of incidence (AI) of the surgical corridor to the petrous carotid, defined as the medial angle between the paracoronal plane passing through the petrous carotid axis and the axis of the surgical corridor. This measure was obtained for 3 different corridors, as follows (fig. 1):

- Contralateral transnasal corridor: the axis passing through the anterior genu of the ICA and contralateral nostril (contra-AI);
- Ipsilateral transnasal corridor: the axis passing through the anterior genu of the ICA and ipsilateral nostril (ipsi-AI);
- Transmaxillary ipsilateral corridor (Sturmann Canfield procedure): the axis passing through the anterior genu of the ICA and the medial border of the ipsilateral infraorbital foramen (TM-ipsi-AI);

Finally, the difference between the angles of incidence (TM-ipsi-AI vs. ipsi-AI; TM-ipsi-AI vs. contra-AI; ipsi-AI vs. contra-AI) was calculated.

Cadaver dissection study

Two fresh-frozen cadaver heads underwent arterial injection with red-stained silicon and a CT scan with 1-mm thickness, neuronavigation acquisition. The dissection was performed with Störz Spice System and a 0° telescope (Karl Störz GmbH & Co., Tuttlingen, Germany). ICAs were exposed bilaterally by endoscopic dissection from the parapharyngeal space up to the intracranial compartment with preservation of vidian nerves. Bilaterally, the transmaxillary ipsilateral corridor was obtained using a Sturmann-Canfield procedure (removal of the anteromedial angle of the maxillary bone from the floor of the nasal cavity

inferiorly up to the infraorbital foramen supero-laterally). The contralateral transnasal corridor was achieved by resecting the posterior half of the nasal septum to entirely visualize the contralateral ICA.

The relationships between the vidian nerve and the anterior and posterior genu of the petrous carotid were evaluated through 3 different angulations:

- Positioning the endoscope in the contralateral nostril (contralateral transnasal corridor);
- Positioning the endoscope in the ipsilateral nostril (ipsilateral transnasal corridor);
- Positioning the endoscope in the ipsilateral nostril after performing a Sturmann Canfield procedure (transmaxillary ipsilateral corridor).

For each access, the inclination of an endoscopic instrument in relation to the target was assessed on axial CT images using an optic neuronavigation system (NDI® Polaris®) and dedicated software (ApproachViewer, part of GTxEyesII).

Quantification of fisheye effect

The fisheye effect was empirically quantified as follows. A picture of a standard metric ruler was taken with a standard camera and a 2D endoscope (4 mm rod-lens Hopkins 0° endoscope, Karl Storz GmbH & Co., Tuttlingen, Germany). The distance from the ruler was arbitrarily set at 5 and 3 cm to mimic the working distance from the target during the phase of parapharyngeal endoscopic dissection. A frame from each distance was recorded.

In each frame the number of pixels included in a distance unit at midline and at the periphery of the picture was calculated using Photoshop CS6. The ratio between the pixels in the peripheral distance unit and the pixels in the midline was called the “distortion ratio” (fig.2). This parameter simply expresses the compression of the distance moving from the center toward the periphery, which is due to the fisheye effect.

Statistical analysis

Data were collected in Excel® (Microsoft®, USA) and analyzed with XLSTAT® (Addinsoft®, USA). Shapiro-Wilk normality and Levene homoscedasticity tests were applied to all measured and calculated data. Contra-AI, ipsi-AI, and TM-ipsi-AI were compared using a one-way ANOVA with Tukey's post-hoc test. The associations between PCA and AI, as well as between PCA and the gain of AI among different corridors, were investigated by Spearman's correlation test. Level of significance was set at 0.05.

Results

All patients were adults (mean age 46.8 years, range 22-64) and were equally distributed for gender (10 males and 10 females). Mean, range, and confidence intervals of the measured and calculated angles are reported in Table 1. The mean PCA was 31°, with a 20° range of variations (21–41°). The intra-individual difference of PCA (i.e., the difference between the PCAs of the two sides in the same patient) was 3° (range, 0–9°). Among the different angles of incidence, TM-ipsi-AI constantly showed the highest values, and ipsi-AI had higher values than contra-AI. These differences were statistically significant (ANOVA and Tukey's post hoc test: $p < 0.0001$).

The relationship between PCA and AIs is outlined in fig. 3. As expected, the value of PCA significantly influenced the value of each AI ($p < 0.0001$). In particular, an inverse proportional relationship was found: higher PCA was associated with lower AIs (fig.3A).

Conversely, the PCA did not impact on the differences of AI among different corridors ($p = \text{ns}$). Thus, the transmaxillary (Sturmann Canfield) approach assured the highest values of AI whatever the value of PCA (fig.3B).

In fig. 4, the impact of different surgical corridors (i.e., different AIs of the endoscope) on endoscopic visualization of the vidian nerve and ICA is shown. In addition, the different angles of incidence of endoscopic scissors in relation to the parapharyngeal carotid segment can be visually appreciated and were confirmed by the navigation system.

Empiric quantification of the fisheye effect is reported in fig. 2. In the 3 scenarios (standard camera, 5 cm [fig. 2A], 2D endoscope, 5 cm [fig. 2B], 2D endoscope, 3 cm [fig. 2C]), the distortion ratio was 0.99 (almost none), 0.84, and 0.63 (maximal recorded distortion), respectively.

Discussion

In the last decade, several dissection studies have focused on the anatomy of the infratemporal fossa, parapharyngeal space, and nasopharynx, as viewed through the endoscopic transnasal approach. These studies paved the way to expand the indications of TES.

The ICA has been one of the most studied targets.⁸ In fact, its rupture can be considered one of the most dramatic complications in endoscopic skull base surgery. Its incidence ranges from less than 1% to 9%⁹⁻¹¹ and is likely to be underestimated because several events may not be reported.¹² Injury of the ICA may result in death (mortality rate of 10%) or cause acute and late neurological morbidity by ischemic injuries (hypoperfusion, thrombosis, or embolism), pseudoaneurysm, and carotid cavernous fistula.¹³ Moreover, management of such massive arterial bleeding in the narrow surgical field of an EEA is challenging; urgent angiography and neuroradiological interventions, such as stenting, coil embolization, or balloon occlusions, are often required.^{12,14,15}

When working in close proximity to the ICA, multiple factors must be carefully considered. First, careful evaluation of pre-operative imaging is mandatory. Critical anatomic variants include pneumatization of the sphenoid sinus, bony septations inserting on the carotid protuberance, thickness of the bone surrounding ICA, and length and course of ICA segments. In case of tumor resection, the relationship between the lesion and ICA must be carefully evaluated. Finally, during surgical dissection, the presence of adhesions should be foreseen in case of previous surgery and/or radiotherapy.¹²

ICA and different endonasal endoscopic perspectives

Different anatomic studies have focused on the identification of reliable landmarks for ICA and its segments. The vidian nerve and medial pterygoid lamina were recognized as indicators for the anterior genu of the petrous ICA,¹⁶ whereas the lateral pterygoid lamina, Eustachian tube, mandibular nerve, middle meningeal artery, and spina sphenoidalis were identified as landmarks for the posterior genu and parapharyngeal ICA.^{7,8,17-20} However, none of these studies analyzed the variability introduced by the different endoscopic perspectives of diverse surgical corridors.

In this study, the angle of incidence of the surgical corridor indicates the inclination of the endoscope in relation to the petrous carotid axis. This angle reveals how the surgeon can perceive the three-dimensional anatomy of the ICA (i.e., the spatial relationship between the anterior and posterior genu). In fact, when the AI approaches zero, the endoscope tends to be parallel to the petrous carotid axis. In that situation, the posterior genu tends to be aligned behind the anterior. Conversely, when the AI increases, the surgical corridor tends to become perpendicular to the petrous carotid axis, and the spatial relationship of the two genu can be better appreciated (the first being posterior and lateral to the second genu).

The practical meaning of these geometric concepts is summarized in fig. 4, which exemplifies how the same anatomical landmark (i.e., the vidian nerve) can acquire a different relevance according to the surgical corridor, through which it is visualized. In case of a contralateral transnasal corridor (low angle of incidence), the posterior genu tends to be hidden behind the anterior one; the parapharyngeal, petrous, and paraclival tract of ICA almost form a straight line. Consequently, the vidian nerve points to both the anterior and posterior genu. Conversely, with an ipsilateral transnasal or trans-maxillary corridor (higher angle of incidence) the lateral position of the posterior genu with respect to the anterior becomes more evident, and the petrous ICA is more clearly identifiable. In this setting, the vidian nerve is a reliable landmark for the anterior genu.

Accordingly, the neuronavigation system (fig. 4 – inferior band) demonstrates that the same surgical maneuver relying on the same landmark (i.e., cutting with the scissors below the vidian nerve as a safe point with regard to the parapharyngeal ICA) can have a different

safety profile depending on the surgical corridor adopted. In fact, the trajectory of the forceps heads for the parapharyngeal ICA in the contralateral nostril approach, while it leads to a region that is slightly medial or far medial to the ICA in an ipsilateral and transmaxillary approach, respectively.

Thus, higher values of AI are related to better visualization of the ICA and greater reliability of its landmarks. The AI is influenced by the PCA and type of approach. PCA and AI are linked by an inverse proportional relationship: the bigger the first, the smaller the second. Thus, high values of PCA are unfavorable, because they tend to determine adverse visualization of the ICA. The trans-maxillary approach (Sturmann-Canfield procedure) always leads to higher values of AI than the ipsilateral approach, and the latter does the same with respect to the contralateral corridor.

The “fish-eye effect”

The fish-eye effect further emphasizes the perspectival changes due to the AI of the surgical corridor. The term “fisheye effect” was coined in 1906 by the American physicist and inventor Robert W. Wood based on how a fish would perceive an ultra-wide hemispherical view from beneath the water. Its empiric quantification reported in fig. 2 clearly defines its practical relevance. The fish-eye effect varies in intensity according to the distance to the target, but it is always present because it is intrinsic to the adopted device. In the extreme situation (fig. 2C), in the periphery of the optic field compression of the distance as high as 37% is observed. As a consequence, structures that are away from the center of view appear closer on the screen than they actually are. Moreover, with a 2D-endoscope the lack of depth perception can further hinder correct rendering of the surgical field on the screen. For example, if we place the anterior genu in the center of the endoscopic view, the visualization of the posterior genu on the screen could be jeopardized by a loss of perception of both its lateral position (due to a low AI of the surgical corridor adopted and/or the fish-eye effect) and its posterior location (caused by the two-dimensional endoscopy).

Practical implications

These data can lead to several technical considerations when approaching lateralized lesions in close relationship with ICA. First, the value of PCA should be always estimated on preoperative imaging. Next, in an EEA via a 2-nostril 4-handed technique, during the most critical phase of the dissection it is advisable to place the endoscope and the instrument for dissection in the nostril that is ipsilateral to the lesion, i.e. using the corridor with the best AI, which provides a reliable visualization of anatomical landmarks and possibly safer trajectory of surgical instruments (fig. 4).

Interestingly, a higher incidence of injury on the left ICA is reported in the literature.¹³ In particular, in the retrospective analysis of the Pittsburgh group on ICA lesions during EEAs, 5 of 7 (71%) ICAs injured were on the left side.⁹ The surgeon causing the injury was always right-handed. The site of injury was the paraclival tract in 2 cases and the paraclinoidal, cavernous, and lacerum tract in 1 case each. It would be interesting to know in which nostril was the endoscope positioned when the injury occurred. In fact, when a right-handed surgeon approaches a left ICA during a two-nostril four-handed technique, it is likely that the endoscope is inserted in the right nostril and surgical instruments in the left one. As demonstrated above, this setting can have a detrimental effect on field visualization and could hypothetically explain (at least partially) the higher prevalence of injuries on the left side.

Finally, in case of high values of PCA, when the tumor has a critical relationship with the parapharyngeal or petrous ICA a transmaxillary Sturmann-Canfield approach might be considered to achieve the best possible AI and potentially reduce the risk of vascular injury.

Limitations of the study

This experimental study presents some limitations. We focused only on the vidian nerve and foramen lacerum as anatomical landmarks of the ICA, because in order to achieve complete ICA exposure many other structures (pterygoid laminae, Eustachian tube) had to be removed. The movements of the endoscope during surgery were not considered.

Endoscopic surgeons usually move the scope “in and out” of the nasal cavities to collect spatial information and bypass the lack of depth perception due to two-dimensional visualization. However, if we focus on the specific and crucial phase of the procedure (e.g. dissection of the parapharyngeal space close to the ICA), these movements have very marginal importance. In fact, the endoscope tends to be steady and very close to the target in order to optimize the visualization.

Lastly, the different corridors were analyzed as straight lines. The AI of a surgical corridor is substantially defined by the fulcrum where the optic lays (i.e., the upper part of the nasal aperture) and the target (i.e., the paraclival ICA), while movement of the endoscope within the same surgical corridor has a very slight impact on AI. For this reason, with the aim of creating a simplified model that could be studied geometrically, we reduced the three-dimensional shape of the surgical corridor (which is similar to a cone with the apex at the fulcrum) to a straight line.

Conclusions

This anatomical study documented the variability of the petrous carotid angle and its importance, together with the surgical corridor adopted, in determining the angle of incidence of the endoscope and dissection instruments on the internal carotid artery. An optimal AI provides reliable visualization of anatomical landmarks and possibly safer use of dissection instruments.

REFERENCES

- 1) Kassam A, Snyderman CH, Mintz A, Gardner P, Carrau RL. Expanded endonasal approach: the rostrocaudal axis. Part I. Crista galli to the sella turcica. *Neurosurg Focus* 2005; 19(1): E3.
- 2) Kassam A, Snyderman CH, Mintz A, Gardner P, Carrau RL. Expanded endonasal approach: the rostrocaudal axis. Part II. Posterior clinoids to the foramen magnum. *Neurosurg Focus* 2005; 19(1): E4.
- 3) Kassam AB, Gardner P, Snyderman C, Mintz A, Carrau R. Expanded endonasal approach: fully endoscopic, completely transnasal approach to the middle third of the clivus, petrous bone, middle cranial fossa, and infratemporal fossa. *Neurosurg Focus* 2005; 19(1): E6.
- 4) Castelnovo P, Dallan I, Bignami M, Battaglia P, Mauri S, Bolzoni Villaret A, et al. Nasopharyngeal endoscopic resection in the management of selected malignancies: ten-year experience. *Rhinology* 2010; 48(1):84-9.
- 5) Ong YK, Solares CA, Lee S, Snyderman CH, Fernandez-Miranda J, Gardner PA. Endoscopic nasopharyngectomy and its role in managing locally recurrent nasopharyngeal carcinoma. *Otolaryngol Clin North Am* 2011; 44(5):1141-54.
- 6) Al-Sheibani S, Zanation AM, Carrau RL, Prevedello DM, Prokopakis EP, McLaughlin N, et al. Endoscopic endonasal transpterygoid nasopharyngectomy. *Laryngoscope* 2011; 121(10):2081-9.
- 7) Castelnovo P, Nicolai P, Turri-Zanoni M, Battaglia P, Bolzoni Villaret A, Gallo S, et al. Endoscopic endonasal nasopharyngectomy in selected cancers. *Otolaryngol Head Neck Surg* 2013; 149(3):424-30.
- 8) Labib MA, Prevedello DM, Carrau R, Kerr EE, Naudy C, Abou Al-Shaar H, et al. A road map to the internal carotid artery in expanded endoscopic endonasal approaches to the ventral cranial base. *Neurosurgery* 2014; 10 Suppl 3:448-71.

- 9) Gardner PA, Tormenti MJ, Pant H, Fernandez-Miranda JC, Snyderman CH, Horowitz MB. Carotid artery injury during endoscopic endonasal skull base surgery: incidence and outcomes. *Neurosurgery* 2013; 73[ONS Suppl 2]:ons261–ons270.
- 10) Frank G, Sciarretta V, Calbucci F, Farneti G, Mazzatenta D, Pasquini E. The endoscopic transnasal transsphenoidal approach for the treatment of cranial base chordomas and chondrosarcomas. *Neurosurgery* 2006; 59:ONS50–57 [discussion: ONS50–57].
- 11) Gardner PA, Kassam AB, Snyderman CH, Carrau RL, Mintz AH, Grahovac S, et al. Outcomes following endoscopic, expanded endonasal resection of suprasellar craniopharyngiomas: a case series. *J Neurosurg* 2008; 109:6–16.
- 12) AlQahtani A, Castelnovo P, Nicolai P, Prevedello DM, Locatelli D, Carrau RL. Injury of the internal carotid artery during endoscopic skull base surgery: prevention and management protocol. *Otolaryngol Clin North Am* 2016; 49(1):237-52.
- 13) Chin OY, Ghosh R, Fang CH, Baredes S, Liu JK, Eloy JA. Internal carotid artery injury in endoscopic endonasal surgery: A systematic review. *Laryngoscope* 2016; 126(3):582-90.
- 14) Raymond J, Hardy J, Czepko R, Roy D. Arterial injuries in transsphenoidal surgery for pituitary adenoma; the role of angiography and endovascular treatment. *Am J Neuroradiol* 1997; 18(4):655-65.
- 15) Valentine R, Wormald PJ. Carotid artery injury after endonasal surgery. *Otolaryngol Clin North Am* 2011; 44(5):1059-79.
- 16) Kassam AB, Vescan AD, Carrau RL, Prevedello DM, Gardner P, Mintz AH, et al. Expanded endonasal approach: vidian canal as a landmark to the petrous internal carotid artery. *J Neurosurg* 2008; 108(1):177-83.
- 17) Liu J, Pinheiro-Neto CD, Fernandez-Miranda JC, Snyderman CH, Gardner PA, Hirsch BE, et al. Eustachian tube and internal carotid artery in skull base surgery: an anatomical study. *Laryngoscope* 2014; 124(12):2655-64.

- 18) Ho B, Jang DW, Van Rompaey J, Figueroa R, Brown JJ, Carrau RL, et al.
Landmarks for endoscopic approach to the parapharyngeal internal carotid artery: a radiographic and cadaveric study. *Laryngoscope* 2014; 124(9):1995-2001.
- 19) Falcon RT, Rivera-Serrano CM, Miranda JF, Prevedello DM, Snyderman CH, Kassam AB, et al. Endoscopic endonasal dissection of the infratemporal fossa: Anatomic relationships and importance of eustachian tube in the endoscopic skull base surgery. *Laryngoscope* 2011; 121(1):31-41.
- 20) Bolzoni Villaret A, Battaglia P, Tschabitscher M, Mattavelli D, Turri-Zanoni M, Castelnovo P, et al. A 3-dimensional transnasal endoscopic journey through the paranasal sinuses and adjacent skull base: a practical and surgery-oriented perspective. *Neurosurgery* 2014; 10 Suppl 1:116-20; discussion 120.

Figure 1. Exemplification of PCA and Als. PCA is the angle of inclination of the petrous carotid axis (dashed white line) in relation to a horizontal plane passing through the stylomastoid foramina (white line). Als are the medial angles between the petrous carotid axis and the axis of surgical corridors: transmaxillary ipsilateral corridor (A) in yellow, ipsilateral transnasal corridor (B) in green, contralateral transnasal corridor (C) in light blue.

Figure 2. Empiric quantification of the fisheye effect. In each frame the distance units were set between 7.3 and 7.7 (midline unit) and between 9.5 and 9.9 (peripheral unit). A, picture with standard camera at a distance of 5 cm; B, picture with 2D-endoscope at 5 cm; C, picture with 2D-endoscope at 3 cm.

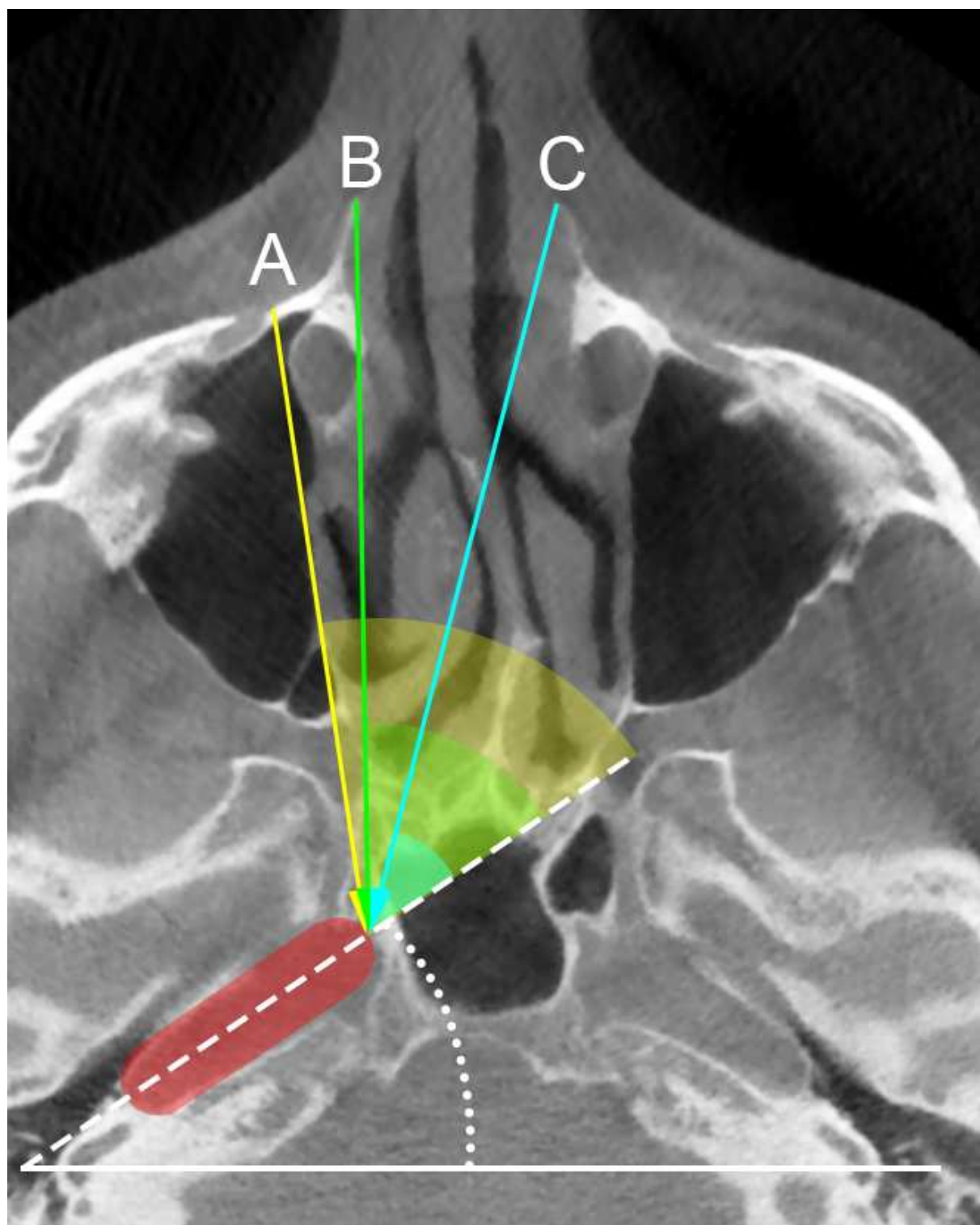
Figure 3. Correlation plot between PCA and the Als. PCA values are reported on the horizontal axis; angles of incidence of the 3 surgical corridors (A) and their differences (B) are on the vertical axis. The black lines express the trends of the values in each group. A: inverse proportional relationship between PCA and Als ($p < 0.0001$ for each AI): the value of each AI reduces (the black lines head downward) while PCA increases. B: absence of correlation between PCA and differences of Als (ipsi-AI vs contra-AI: $p = 0.858$; TM-ipsi-AI vs contra-AI: $p = 0.771$; TM-ipsi-AI vs ipsi-AI: $p = 0.640$). Black lines are horizontal: while PCA increases, the differences of Als are unvaried.

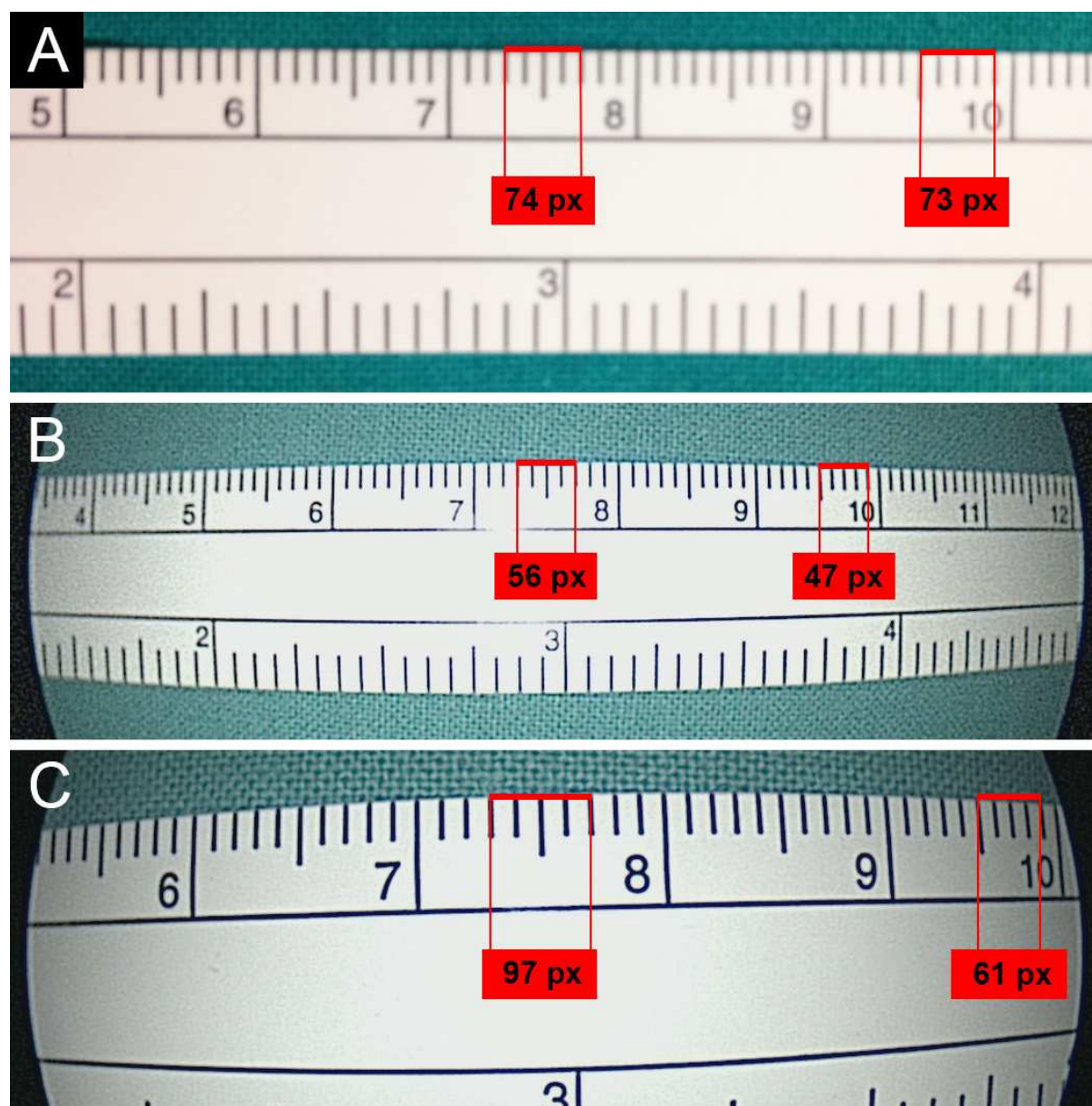
Figure 4. In the superior band, different endoscopic perspectives of the ICA (and in particular of its petrous tract) depending on the surgical corridor adopted (left side, contralateral nostril; middle, ipsilateral nostril; right side, transmaxillary Sturmann-Canfield). The forceps are below the vidian nerve at the level of the foramen lacerum, and thus in a position that is medial to the posterior genu and parapharyngeal ICA. In the inferior band,

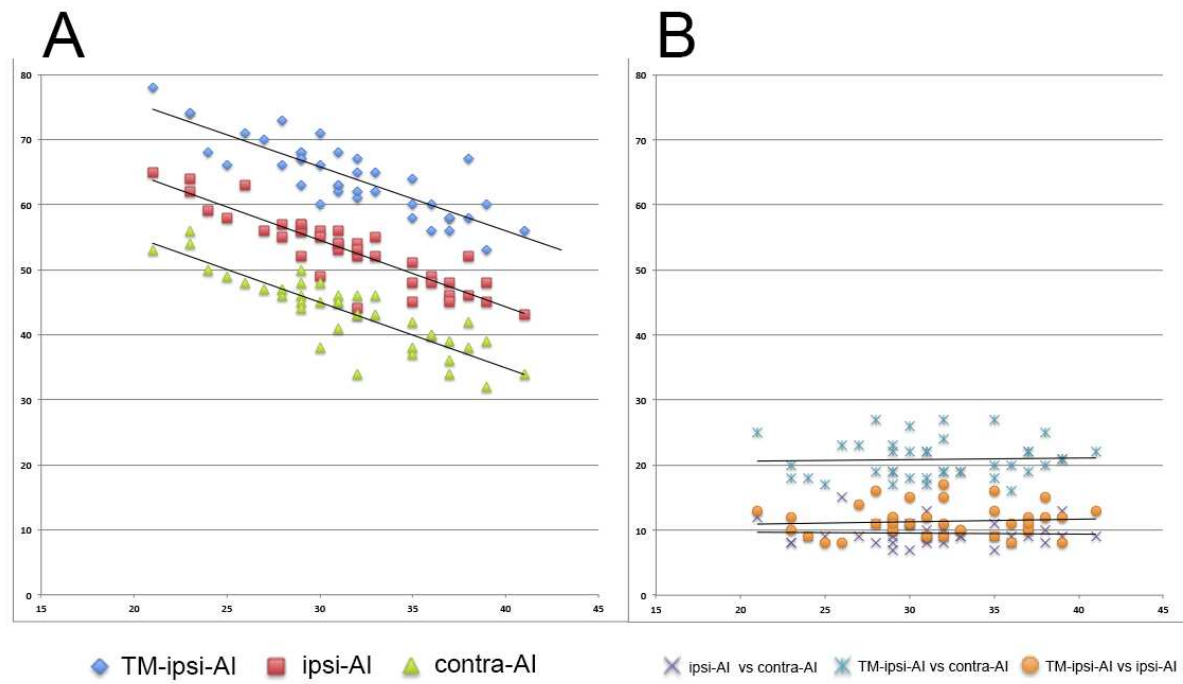
the same pictures are proposed as seen with the optic navigation system. The trajectory of the forceps (yellow line) heads for the parapharyngeal ICA in the contralateral nostril approach. Conversely, it leads to a region that is slightly medial or far medial to the ICA in an ipsilateral and transmaxillary approach, respectively. Legend: AG, anterior genu; PG, posterior genu; pphICA, parapharyngeal internal carotid artery; VN, vidian nerve.

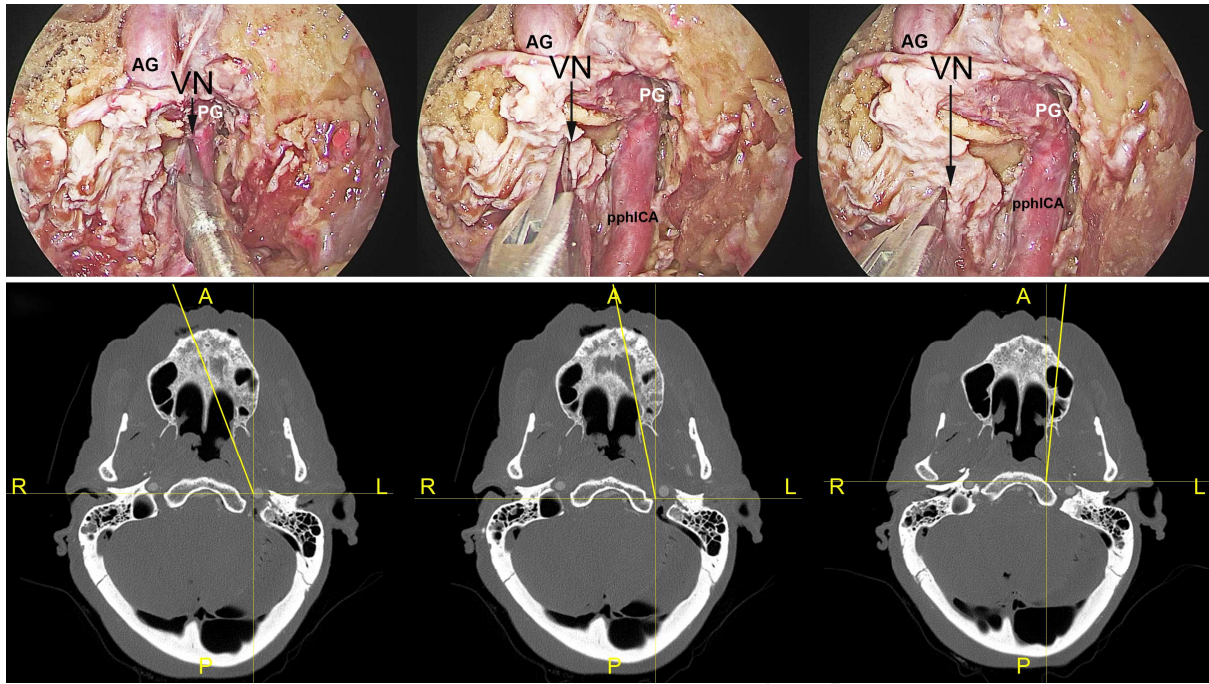
Table 1. Measured and calculated angles.

Angle	Mean (degrees)	Range (degrees)	95% Confidence interval (degrees)
PCA	31	21-41	30-33
Contra-AI	43	32-56	42-45
Ipsi-AI	53	43-65	51-55
TM-ipsi-AI	64	53-78	63-66
TM-ipsi-AI vs. Contra-AI	21	16-27	20-22
TM-ipsi-AI vs. Ipsi-AI	11	8-17	11-12
Ipsi-AI vs. Contra-AI	10	7-15	9-10









Highlights

- An anatomical and radiological study of ICA geometry was performed
- Surgical corridor and fisheye effect can influence the perception of ICA landmarks
- Corridors ipsilateral to the lesion assure a better angle of incidence (AI) on the target
- The better the AI, the more reliable the visualization, the safer the dissection
- Endoscope and instruments for dissection should use an ipsilateral corridor

Financial disclosures and conflicts of interest

Authors have no funding source to declare.

Authors have no conflict of interest to disclose.